Structures 84 (2026) 110981

Contents lists available at ScienceDirect

Structures

journal homepage: www.elsevier.com/locate/structures

Fire resistance of protected glued laminated timber columns: Geometry, load and cladding effect

Paulo A.G. Piloto [a,*], Manuel D. Lorenzo [b], Ana B. Ramos-Gavilán [b], Javier Sánchez-Haro [c], Loïc Lannou [d], Abdelhamid Bouchaïr [d]

[a] GICoS, Instituto Politécnico de Bragança, Bragança, Portugal
[b] Departamiento de Ingeniería Mecánica, Universidad de Salamanca, Zamora, Spain
[c] Departamiento de Ingeniería Mecánica y Estructural, Universidad de Cantabria, Santander, Spain
[d] Université Clermont Auvergne, Clermont Auvergne INP, CNRS, Institut Pascal, Clermont-Ferrand, France

ARTICLE INFO

Keywords:
Fire
Glue Laminated Timber
Gypsum protection
Columns

ABSTRACT

Timber, as a sustainable and renewable building material, is becoming increasingly popular in modern architecture due to its aesthetic appeal, low environmental footprint, and structural ability. Glued-laminated timber (GLT) is commonly used for columns and beams in mid to high-rise buildings due to its strength and spanning ability. However, concerns about timber's combustibility raise safety concerns that demand the use of effective fire protection materials. One such method is the application of gypsum cladding, which provides thermal insulation and delays heat transfer to the timber, thus enhancing fire resistance. This study investigates the fire resistance of gypsum-protected GLT columns, focusing on the effects of geometry, load level, and cladding configuration. The European Charring Model (ECM) and the effective cross-section design method are used alongside with three experimental tests, full three-dimensional computational model and a parametric study. The results provide valuable insights into the thermal insulation performance of gypsum cladding, the charring behaviour of timber under fire, and the influence of different protection layers and load levels on overall fire performance. Under 36 % load level, doubling the protection layer, increases the fire resistance up to 95 %. Changing the material grade from GL24h to GL28h, increases the fire resistance, from 2 % to 12 %, depending on the slenderness of the column, while increasing the load level from 6 % to 36 % reduces the fire resistance up to 47 %. This research contributes to fire safety and supports the expanded use of engineered timber in sustainable building designs by improving knowledge of its fire performance characteristics.

1. Introduction

As a sustainable and renewable building material, timber has seen a resurgence in modern architecture due to its aesthetic appeal, low environmental footprint, and structural versatility. Glued-Laminated Timber (GLT) is prevalent for its strength and ability to span significant distances. However, timber's combustibility raises concerns about fire safety, especially for load-bearing structural components. In response to these concerns, various fire protection methods have been developed to enhance the fire resistance of timber elements, allowing them to meet stringent building safety codes. One effective technique for increasing the fire performance of GLT columns is by applying protective gypsum cladding. Gypsum plasterboards are widely recognised for their fire-resistant properties due to their ability to insulate and delay heat transfer. When applied around GLT columns, gypsum layers act as a barrier, slowing the temperature rise in the timber and delaying structural degradation.

This manuscript explores the principles and efficacy of gypsum-based fire protection for GLT columns. Especially, the thermal insulation provided by gypsum, the European Charring Model (ECM), the effective cross-section design method, and the implications of various gypsum configurations on the overall fire performance of GLT columns will be presented. Timber is a structural material and is widely available as a sustainable construction material. In US and Europe, many structures, including houses and industrial buildings and structures, are made from timber. Timber is an orthotropic material with different strength and stiffness properties in the longitudinal, radial and tangential directions of the fibers.

* Corresponding author.
E-mail address: ppiloto@ipb.pt (P.A.G. Piloto).

https://doi.org/10.1016/j.istruc.2025.110981
Received 8 August 2025; Received in revised form 17 December 2025; Accepted 18 December 2025
Available online 23 December 2025

Timber design codes with adequate calculation methods are always improving the formulae to better predict fire resistance, as is the case with the evolution from EN1995–1–2 [1], 2004 to the future generation prEN1995–1–2 [2], 2023. The Eurocode EN 1995–1–2 is based on the European Charring Model (ECM) and presents two different simplified design methods. The main difference between the current version and the future version is related to the ECM, the introduction of tabulated values, the improvement of the effective cross-section method, the exclusion of the reduced properties method, the inclusion of design rules for cross-laminated timber, the improvement of design rules for timber structure subsystems, the inclusion of design rules for wood-concrete composite elements, the introduction of the compartmentalisation function method and the improvement of connection sizing rules.

The design method is based on the charring rate of the timber, considering its surfaces exposed to fire. The position of the char-line should be taken as the position of the 300 ºC isotherm [1]. The combustion can therefore only start if there is a sufficiently powerful external heat source and it is applied for a sufficiently long time to start the pyrolysis phenomenon. The combustion of the first particles released generates energy, which is radiated towards the surface, allowing the pyrolysis of other solid particles, which, in turn, will undergo combustion. It is also understood that, for a given material, if the pyrolysis rate is constant, the speed of propagation of the pyrolysis front towards the inside is lower when the material is denser.

The mechanical properties of timber elements are significantly reduced, even for a temperature increase of only 100 °C. The tensile strength, for example, falls almost linearly to zero when the temperature rises to 300 °C [1]. In compression, the fall is even faster. According to EN1995–1–2 [1], the strength and modulus of elasticity for softwood in the grain directions should be multiplied by a temperature-dependent reduction factor. For compression perpendicular to the grain (orthogonal directions), the same strength and stiffness reduction factors can be applied, which is not physically correct and a reason to explore the orthotropic behaviour in the current computational investigation. These relationships include the effects of transient creep of timber [1]. The material investigation conducted by [3], with respect to wet and dry wood at elevated temperatures, shows that compression properties mainly depend on lignin. The compression strength would decrease with temperatures between 100 and 160 ºC, then there should be an increase 160–210 ºC due to strength gained by drying and finally, a decrease with temperatures between 210 and 280 ºC. This behaviour is not included in our investigation, and the monotonous decrease is considered. According to these authors [3], in room temperature conditions, dried samples were approximately 70 % stronger than samples with a moisture content of 12 %. Regarding the elastic modulus and at room temperature, the effect of moisture was observed to be insignificant. At temperatures approaching 100 ºC, however, the moisture substantially reduced the elastic modulus due to wood softening. After 100 ºC the heated moist samples would dry up and start to increase the elastic modulus, followed by a decrease at higher temperatures.

Previous investigations about the compressive behaviour of unprotected timber columns may be found in the research developed by [4], where six columns were tested under high temperatures. All columns had the same length 1.8 m. The research involved two different cross-sections (different slenderness). The furnace temperature was determined by a single burner using a manual control process. The test was continued until a failure took place when the column was no longer capable of holding the applied load. The tested columns failed due to global flexural buckling, and none of the six tested columns experienced any expansion. Typical contraction displacement is presented over time. The fire resistance of these unprotected columns decreased with load level and slenderness, as expected, but in a less pronounced way when compared to the current protected columns, used in this investigation, when using similar slenderness and material strength. The authors did a comparison of experimental data with the simplified method (effective cross-section method), and results showed a reasonable agreement with the fire resistance of EN1995–1–2 being on the safe side by an average safety factor of 38.7 %. The experimental results of our investigation (protected columns) present a smaller safety factor, depending on the Eurocode version (+23 % for the current version and +19 % for the second generation). It is worth mentioning that a 10 % unsafe result was found for the case of the smaller load level, when comparing the experimental results to the second generation.

[5], developed a numerical model, considering the effect of the moisture and char formation on the buckling behaviour of timber columns under fire. The heat and water (liquid and gas phase) equations were solved using the finite-difference method, and the buckling load was determined using a linearised buckling method. The research process was developed in three steps. The first step was the fire model, the second was the thermal and mass (water) transfer model, and the last was dedicated to the structural model. According to these authors, the highest temperature gradients in the unburnt timber are located at the char line. The unburnt timber close to the char line will experience thermal degradation and thus lose its strength and stiffness properties. Increasing the initial water content increases the reduction factor (increasing the load-bearing capacity). The residual area also decreases with fire exposure time, and this relation is non-linear. The results of this method present higher fire resistance, in most cases (with and without water), when compared to the current version of EN1995–1–2, except for the smallest load level (20 %) and for the case of neglecting the water effect.

[6] presented an interesting comparison of five different failure criteria with the experimental results obtained from two-dimensional mechanical behaviour of timber elements. The limitations of each failure model (Hill, Tsai-Hill, Tsai-Wu, Hoffman and Norris) were presented. All values generated relatively similar envelope failure curves, except for the Norris criterion. According to our simulations, when using the Hill criterion, the failure criterion is not decisive with respect to the calculation of the fire resistance of GLT columns, but it is decisive for the simulation developed at room temperature to determine the load bearing capacity.

The Hill criterion [7] is based on von Mises's theory and adapted for orthotropic materials. Hill's criterion considers the interaction between the stress in the failure mechanism and depends on the orientation of the stress with respect to the orthotropic axis of the material. This criterion allows the determination of the elastic and elastoplastic zones in the stress-strain relationship of the wood. The characteristic parameters of the orthotropic material, defined for this criterion, are the R_{ij} yield rates, which are established as a function of the limit stress in the main directions of the material. Assuming that the wood does not have the plastic capacity, the elastic perfectly plastic regime is considered for the constitutive law in this investigation, just to check that the material remains within the elastic limit.

The type of adhesive affects the fire resistance, as reported several years ago by [8]. The fire resistance was tested on four different types of adhesives (phenolic, resorcinol, urea, and casein), using different types of wood species, and they concluded that casein appeared to decompose at lower temperatures and observed some delamination during the tests before the laminates had been completely charred. The fire resistance of glue-laminated casein specimens was found to be 20 % lower than that of glue-laminated phenolic specimens. More recently, in our research group at IPB, [9] investigated the adhesion properties of bonded joints of medium-density fibreboard and pinewood panels using resins based on urea and resins based on polyurethanes derived from diphenylmethane diisocyanate (MDI). The authors also used three different fire-retardants. Tear failure mode was observed for all cases at room temperature and 100 °C. At elevated temperatures, the adhesives lose strength at 200°C and 230 °C, and the cohesive failure mode becomes the predominant mode. The MDI-based resin showed higher shear resistance at elevated temperatures compared to the urea-based resin. At elevated temperatures, the shear strength of the MDI-based resin decreased by approximately 50 % at 200 °C, while the decrease for the

urea adhesive was 98 %. The addition of 4 % and 2 % of Ammonium polyphosphate (APP) (fire retardant) to MDI base resin improved the shear strength at 100 and 200 ºC, respectively. The fire-retardants did not enhance shear strength at 100 °C for the urea cases.

[10] introduced the burnout resistance of timber columns, assuming an incremental and iterative thermo-mechanical numerical analysis, following a natural fire curve (parametric) to determine the failure time of the timber column. This failure time is related to the minimum duration of the heating phase (ISO834 heating stage of the curve). The burnout resistance of the columns was found to be 20–50 % of their standard fire resistance. The numerical model was defined using SAFIR, with 2D planar finite elements for the thermal analysis (not considering the heat flow by conduction over the length of the column) and 3D beam finite elements for the thermo-mechanical analysis. This model is much simpler than the one it is presented in the current investigation.

More recently, [11], proposed a new method for assessing the structural adequacy of timber columns under fire, considering the loss of strength due to both charring and thermal degradation of timber behind the char layer. This methodology is especially important for the case of natural fires, but also applicable for standard fires when flames are extinguished. This method considers that the thermal penetration continues to reduce the strength and stiffness as the fire decays, and that the thermal degradation is not a fixed depth and changes with heating and cooling during fire exposure. According to these authors, the term "thermal degradation depth" has been defined as the zone of permanently reducing structural capacity based on the 120°C isotherm. This threshold limit is very important because it allows reversing the mechanical properties during cooling. From the CodeRed experiment, the authors verified that if the end of flaming was taken as the time of charring, 15 mm of charring would not have been accounted for, leading to unsafe fire resistance ability.

[12] used ABAQUS to simulate a full 3D solid finite element model, suitable to consider the temperature-dependent thermophysical properties and the development of char layer effect over time. The model used a one-way sequential coupling of thermal analysis with thermo-mechanical analysis. The thermal analysis used an incremental and iterative solution method, while the thermo-mechanical analysis used an elasto-plastic model with nonlinear hardening, assuming the orthotropic behaviour of the timber element. The model accurately predicted temperature, displacements, and the depth of the charred layer, helping to predict the fire resistance of softwood timber elements. The numerical model was validated using Laminated Veneer Lumber (LVL) elements under tension load and bending moment. This model is closer to the current 3D model developed in this investigation, but does not include any failure criterion.

[13] investigated the effect of the charring rate and residual bearing capacity of glulam columns made from six commonly used wood species (C45 Larch from a third country, C40 Canadian Douglas fir, C30 Chinese poplar, C24 Canadian hemlock, C22 European spruce, and C18 Chinese fir). The columns were exposed to two different fire scenarios (one-sided and two-adjacent-side fire exposure). The heat-resistant adhesive was based on phenol–resorcinol–formaldehyde (PRF), demonstrating higher thermal resistance than wood between 20 and 280 °C (but higher conductivity). The adhesive had a spot life of 35 min. Temperature measurements at an exposure depth of 12 mm revealed that Douglas fir, poplar, hemlock, and spruce experienced charring temperatures between 10 and 13 min, whereas larch from the third country and Chinese fir reached this temperature after 30 min. This can be justified by the difference in wood densities and lignin content. In the current investigation, the columns were protected by the four sides and the thermocouple S2 (located at 12.5 mm) never reached the charring temperature. Wood species with high lignin content (European spruce and Chinese fir) generated more solid residue at elevated temperatures. The results showed that high-density glulam columns always have lower charring rates.

[14] made an experimental test and used numerical methods to characterise the progressive damage of a 2D portal frame made by GLT, assessing the robustness when submitting the central timber glued laminated column and the connected glued laminated beam to a localised fire. The authors found a difference of 1 min between the failure time of the central column and the collapse time of the 2D portal timber frame. The results also demonstrated that losing the central column induced a catenary effect over the beams that justified the 2D timber frame failure, which reflects the importance of analysing the fire resistance of protected GLT columns.

More recently, [15], proposed an alternative advanced solution method, based on the equivalent temperature to produce the same strength and stiffness on timber columns. This method simplifies the traditional one-way sequential analysis, allowing the use of a 2D thermal analysis, converting the temperature field into two uniform temperature values (one for compression strength (*Tr*) and the other for bending stiffness (*Te*)). The second step requires the 3D mechanical simulation using the Timoshenko finite element beam (ABAQUS), assuming the stress-strain curve to be elastic, perfect plastic with the definition of the yielding point. The determined *Tr* and *Te* are included into the 3D beam model to determine the displacement over time, after the introduction of the target load. This model simplification reduces the computing effort with respect to the current investigation, but tends to overestimate the fire resistance when using the charring temperature of 300 ºC, with respect to experimental test and to the full 3D finite solid element (ABAQUS).

Different protection systems may be used to increase the fire resistance. [16], presented a manufacturing method to produce a fire-retardant plywood cladding method for the protection of timber elements, as an alternative to gypsum cladding. [17], tested two protection options on two LVL columns (180×180 mm^2 and 180×400 mm^2). The authors also tested the same unprotected cross-sections. Different protection options have been tested, using a 10 mm thick glass–magnesite layer, a 12.5 mm thick fire-resistant gypsum cardboard (FRGP) layer, and a 20 mm thick mineral wool layer. The protection option 1 used the combination of (10 +12.5 +12.5), while protection option 2 used the combination of (20 +20 +10 +12.5 +12.5). The fire protection option 1 led to an increase of 84 % (+26 min) and fire protection option 2 led to an increase of 142 % (+44 min), when testing the smallest LVL cross-section. These numbers were modified to an increase of 79 % (+34 min) for fire protection option 1 and 107 % (+46 min) for the fire protection option 2, when using the largest LVL cross-section. The authors also applied the simplified method and the advanced calculation method (using ANSYS 2D thermal analysis, only). The simplified method overestimated the fire resistance, and the advanced calculation method overestimates and underestimates the experimental results, demonstrating the need to develop more investigation on protected columns.

This investigation presents the results from the experimental tests, using two different protection levels and two different load levels, conducted according to the standard fire test EN1363–1 [18] and EN1365–4 [19]. The research also includes a 3D Solid finite element model to simulate the elastic buckling, load-bearing at room temperature, the fire-exposed thermal analysis and the final thermo-mechanical analysis to determine the fire resistance. The numerical model is validated, comparing the temperature evolution, the displacement over time and the char layer evolution. A parametric analysis is also presented to verify the effect of the cross-section size, column length, material grade and protection level. The two versions from the EN1995–1–2 (2004 and 2023) of the simplified model are also used to compare the results. This investigation bridges the gap between a full 3D model and the simplified models, using orthotropic and non-linear material properties, validated with experimental results. This study explores the principles and efficacy of gypsum-based fire protection for GLT columns. It focuses on the thermal insulation effect, the application of ECM, and the effective cross-section design method. Through design assisted by testing, simulations and simple design rules, this study aims

Table 1
Tested specimens used for validation and verification. (a) experimental results according to EN1363-1 [18] and EN1365-4 [19]; (b) GMNIA ANSYS results; (c) EN1995-1–2 results [1]; (d) prEN1995-1–2 results [2]. The fire resistance in [min].

Specimen	Load [N]	Layers/ thickness [mm]	Failure mode	Fire resistance (EXP) (a)	Fire resistance (NUM) (b)	Fire resistance (EN1995-1–2) (c)	Fire resistance (PrEN1995-1–2) (d)
Sp1	36609	1/ 12.5	Buckling	30	30	30	33
Sp2	10162	1/ 12.5	Buckling	47	40	36	38
Sp3	36609	2/ 12.5	Debonding	36	56	58	61

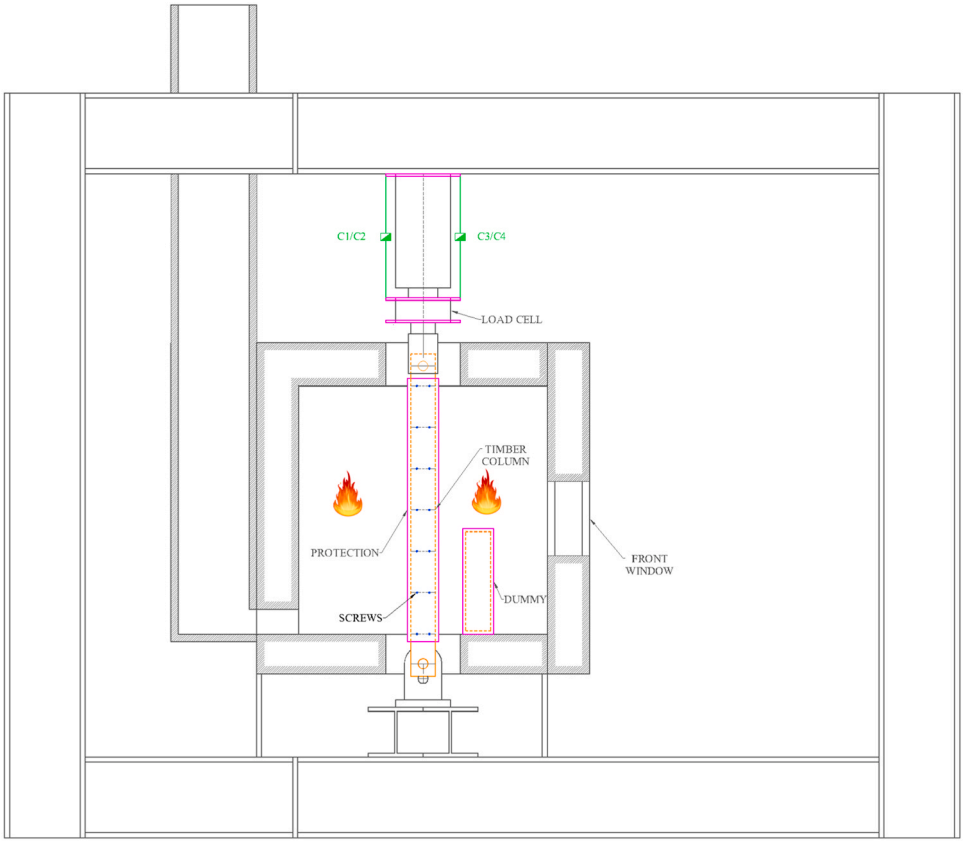

Fig. 1. Testing specimens in the fire resistance furnace.

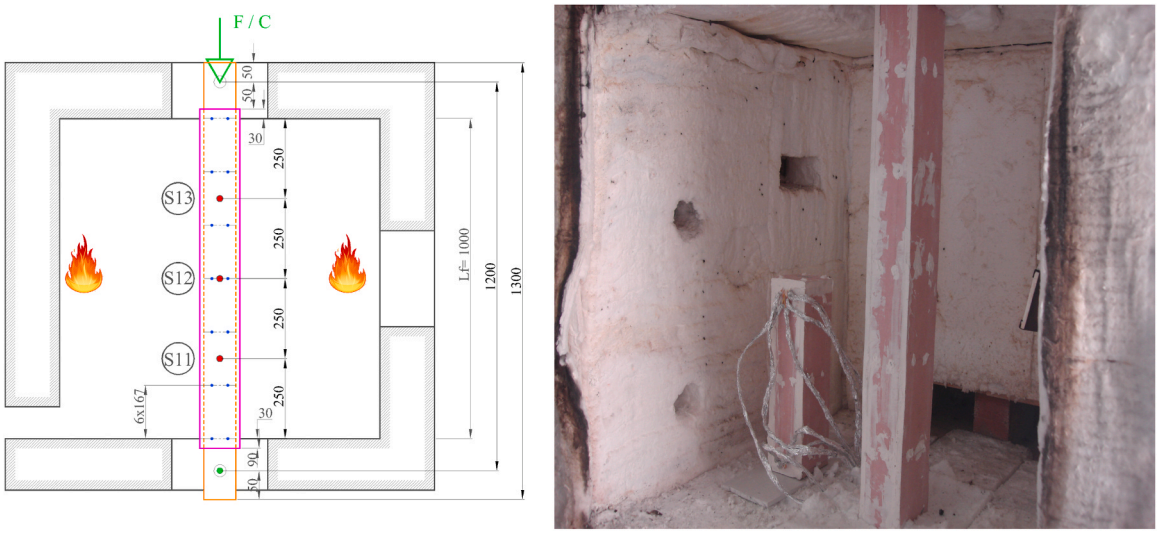

Fig. 2. Thermocouples, screws and position of the specimen inside the furnace.

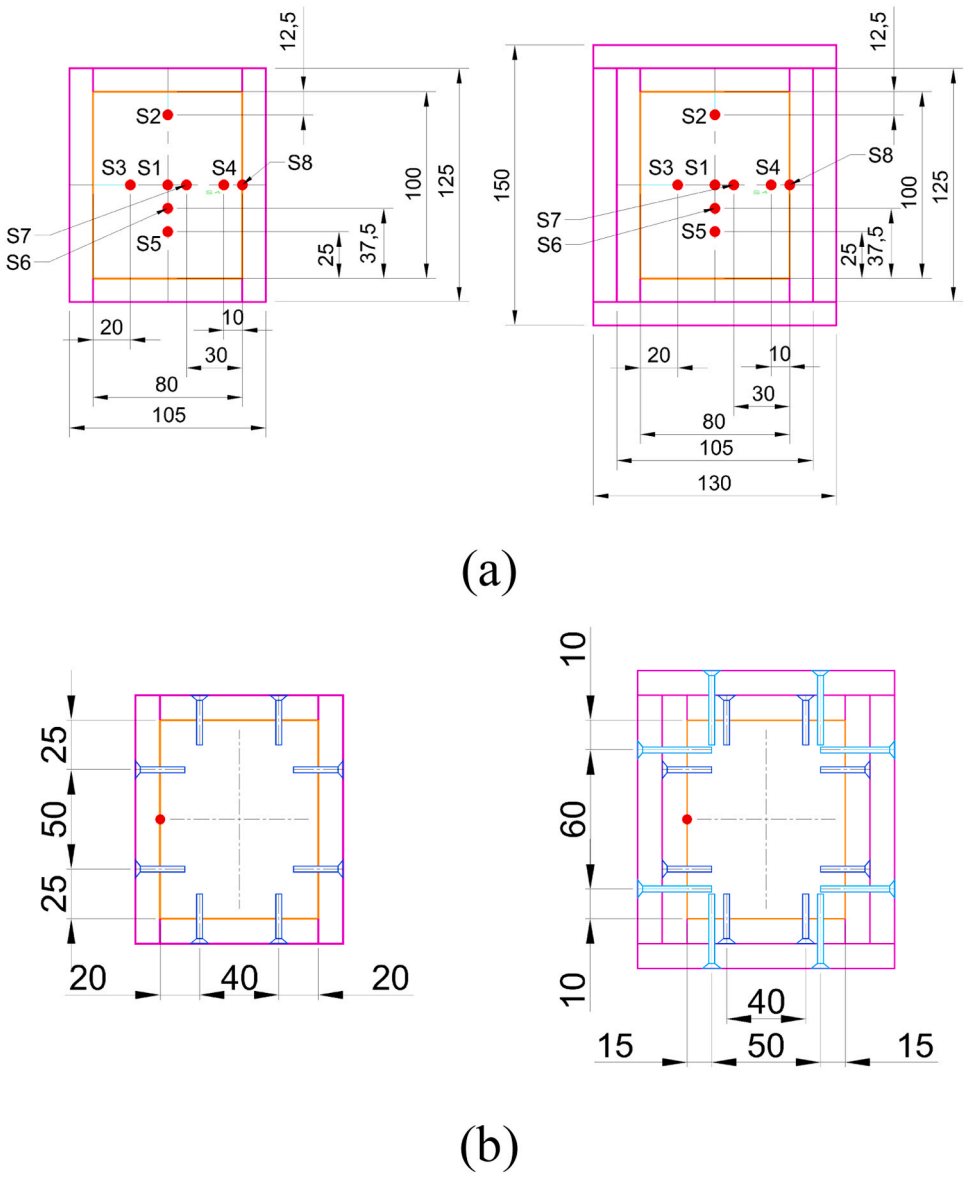

Fig. 3. Thermocouples in the dummy and arrangement of timber protection.

to contribute valuable insights into the fire safety of engineered timber, supporting its expanded use in sustainable building designs.

2. Experimental tests

Three experimental tests were conducted under standard fire conditions. The load level and the protection level were specified according to the fire resistance time predicted by the simplified calculation method, see Table 1. The three specimens (Sp1-Sp3) are made from Spruce Sitka GL24h, produced with CE certification from the German company (Mayr-Melnhof Holz), using a cross-section of 80 × 100 mm^2, and 1.3 m total length, using 1.0 m length exposed to fire, featuring different load levels (6 % and 21 %) and protection levels (one or two 12.5 mm gypsum plasterboard layers).

The experimental setup is presented in Fig. 1. This setup includes the fire-resistance furnace with four burners, each with 90 kW maximum power, running on natural gas. The timber column is pinned at the bottom using a double support and pinned at the top using a double support connected to the hydraulic jack. Both supports are linked to a steel portal frame. The load is applied using the hydraulic jack fixed to the steel portal frame. The load and the reaction are transferred to steel shafts inserted in the previously drilled timber column (40 mm diameter). Four displacement transducers were applied to the top of the moving head of the hydraulics. The load cell will keep the load constant during the tests.

2.1. Specimens and instrumentation

According to EN1365–4 [19], three thermocouples (S11, S12 and S13) were applied to the main specimen to track the interface temperature between the external surface of the timber columns and the internal surface of the gypsum protection layer. These thermocouples are arranged with a spacing of 250 mm (one quarter of the exposed length). The protection layers were attached to the timber column, using screws with a diameter of 3.5 mm and a length of 25 mm and 45 mm, to fix the base layer and the second layer, respectively. A set of two screws was applied every 167 mm, for each face, see Fig. 2.

Temperatures were also measured in a 400 mm small-scale specimen (dummy) in different positions over the cross-section and along the dummy length (S1 to S8). The purpose of using the dummy column was to measure the temperature inside the cross-section for detailed data analysis and validation of the computational model, avoiding affecting

Table 2
Reference for the timber GL24h mechanical properties [20].

Property	Formula	Value [MPa]
Bending strength	$f_{m,g,k}$	24.0
Tensile strength	$f_{t,0,g,k}$	19.2
	$f_{t,90,g,k}$	0.5
Compressive strength	$f_{c,0,g,k}$	24.0
	$f_{c,90,g,k}$	2.5
Shear strength	$f_{v,g,k}$	3.5
Elastic Modulus	$E_{0,g,mean}$	11500.0
	$E_{0,g,05}$	9600.0
	$E_{90,g,mean}$	300.0
	$E_{90,g,05}$	250.0
Property	Formula	Value [kg/m^3]
Density	$g_{g,k}$	385
	$g_{g,mean}$	420

the main column's fire resistance. The thermocouples were inserted in holes with a 5 mm diameter, using different depths to avoid interference during measurements (150, 180 mm, starting from the top and 180 mm starting from the bottom). Fig. 3 presents the position of the thermocouples and the arrangement of the gypsum protection layers, including the screw locations.

Timber columns were made with spruce sitka GL 24 h, with a cross-section of 100×80 [mm^2], including three lamellas, each with 33.3 mm. Table 2 presents the resume of the mechanical properties at room temperature, according to EN14080 [20]. The authors also did a compression test and obtained 26 MPa on compression strength, with the corresponding density of 365 kg/m^3.

The protection material was obtained from Saint Gobain, using Placo PPF13, with a density of 832 kg/m^3, with 12.5 mm thickness, and a fire reaction of Q2-S1, d0. This classification indicates limited combustibility, meaning it doesn't readily ignite or contribute significantly to fire growth. It produces little or no smoke during combustion and does not produce flaming droplets or particles within the first 10 min of a fire. Essentially, it's a fire protection material with a high level of fire safety, especially in the early stages of a fire. The gypsum plasterboard joints of the protection layers were filled with gypsum paste made in the laboratory.

2.2. Observations during tests

During the experimental tests, several photos were taken from the columns with single and double protection. Fig. 4 shows several time frames enabling a comparison between the behaviour of the timber element with a single-layer protection and with double-layer protection. These photos also provide important information regarding the start of the ignition. This ignition event starts from the joints formed between the protective layers and the release of flammable gases. The start of ignition for a single protection layer was achieved at almost the same time (19 min for specimen Sp1 and 18 min for specimen Sp2). There was no ignition for specimen Sp3 corresponding to double protection layers. The photos give a time history during the experimental tests, ending with the last frame corresponding to opening the front door of the furnace.

Taking the specimen Sp1 as reference, when the load is reduced, the fire resistance increases, but the time for ignition remains almost the same. Keeping the load, but doubling the protection level, there is still an increase in the fire resistance, see the behaviour of Specimen Sp3. No ignition has been noticed before the failure of the element, and this specimen Sp3 suffered from a different failure mode (lamellas debonding) on the top of the specimen.

The debonding failure mode was not expected to occur, and this

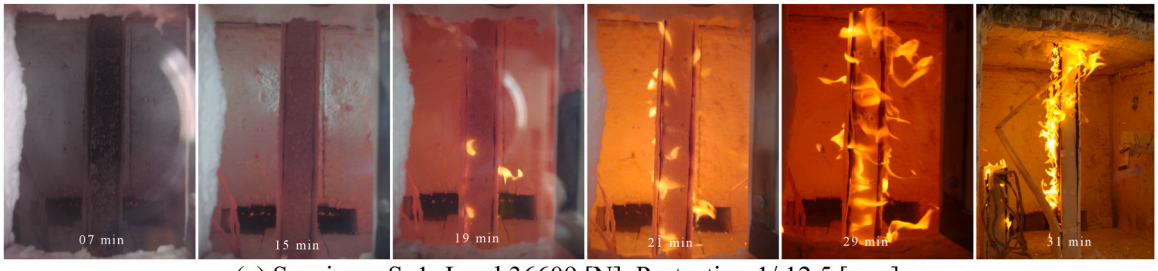

(a) Specimen Sp1: Load:36609 [N], Protection:1/ 12.5 [mm].

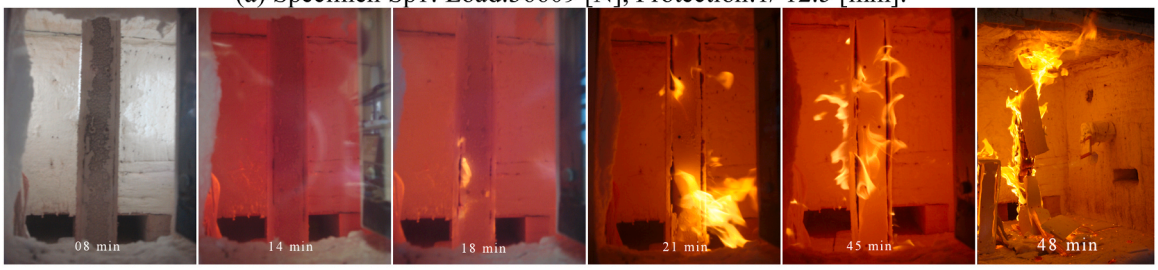

(b) Specimen Sp2: Load:10162 [N], Protection:1/ 12.5 [mm].

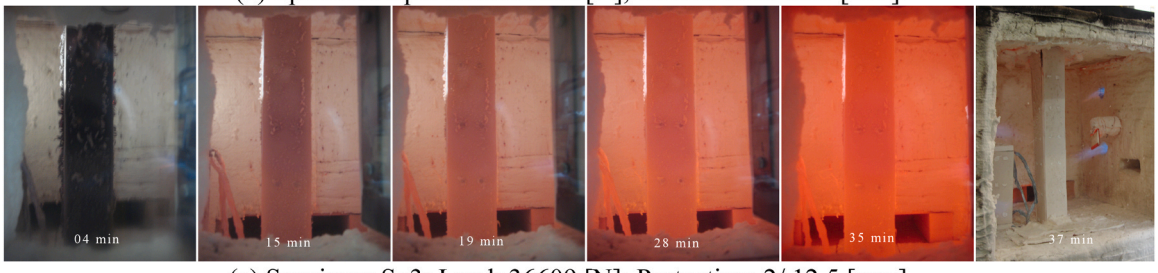

(c) Specimen Sp3: Load: 36609 [N]: Protection: 2/ 12.5 [mm].

Fig. 4. Time frames during and at the end of the experimental tests.

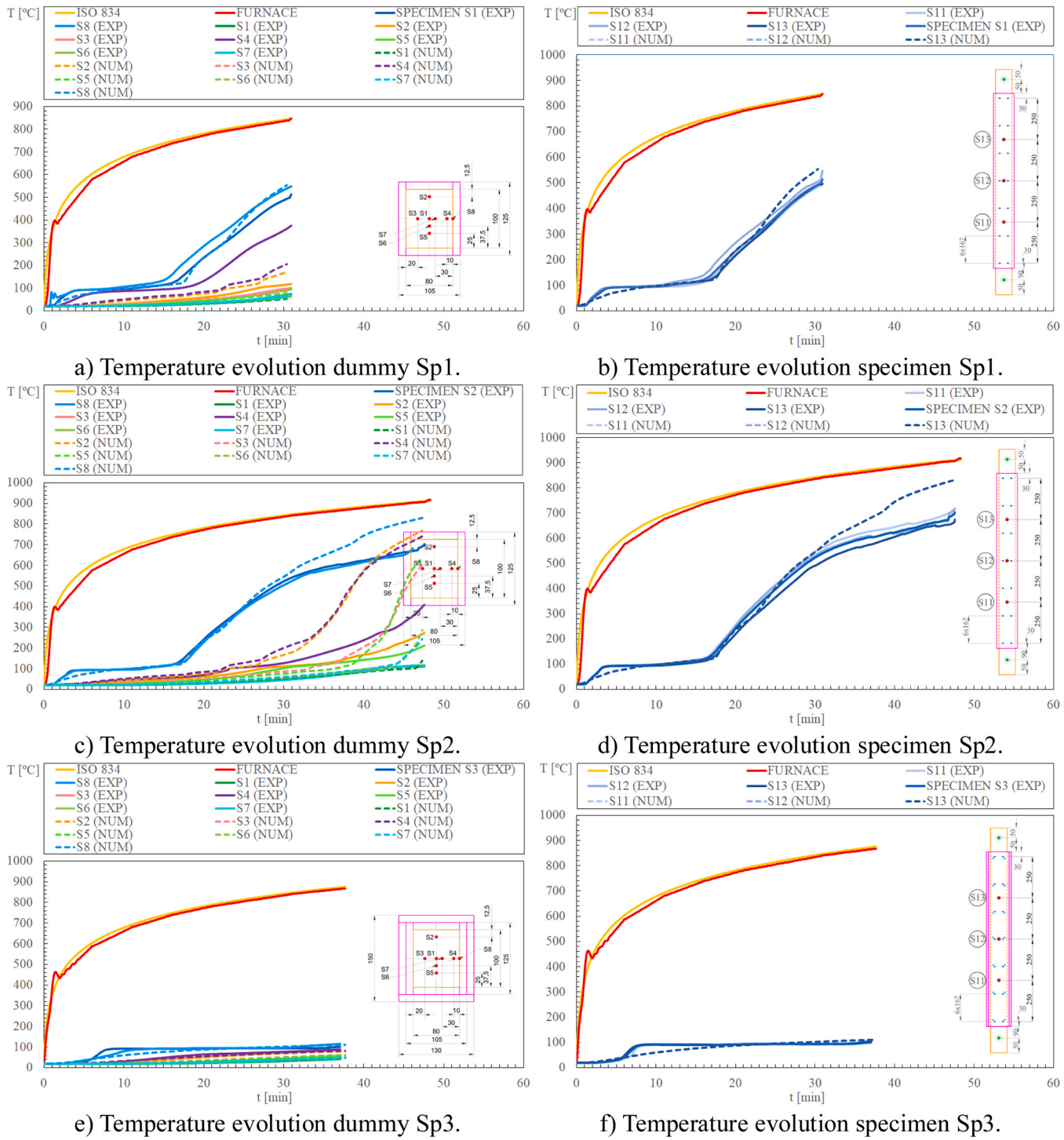

Fig. 5. Temperature evolution in the columns and dummies.

failure may be justified by a deficient insulation on the top support of the column, associated with a stress concentration factor due to the existence of a drilling hole with 40 mm on diamenter aligned with the lamellas (33 mm thickness each). This drilling hole was adjusted by a steel shaft to bear the load at the top support of the column. Depending on the resin used by the GLT manufacturer (based on melamine resin), one can also expect a big reduction of the shear strength, with respect to room temperature, depending on the resin type, Silva *et al.* [9].

2.3. Temperature measurements

Temperatures were recorded in the main elements and on the dummies. A similar trend has been observed for the external surface of the timber column and the external surface of the dummy (compare SPECIMEN S# with S8). The most affected zone for specimen Sp1 was S4 (at a distance of 10 [mm] from the external surface), reaching the 300 °C isothermal after 27 min. The thermocouple S2, which is located inside timber at 12.5 mm from the interface between the timber external face and the gypsum internal face, reached 113 °C maximum at the end of the test (30 min), see Fig. 5.

Table 3
Temperature evolution for all specimens, for the first 30 min. These are the average temperatures for each specimen, determined from S11, S12 and S13 measurements.

Time [min]	Specimen Sp1 (EXP) [ºC]	Specimen Sp2 (EXP) [ºC]	Specimen Sp3 (EXP) [ºC]
5	92	92	28
10	95	97	91
15	114	111	91
20	232	240	91
25	364	395	93
30	486	522	93

The most exposed thermocouple inside the cross-section (S4) from the dummy specimen Sp2 reached the 300 ºC isothermal after 44 min. The thermocouple S2 reached the maximum temperature of 268 ºC at the end of the test (47 min). Apparently, the difference between dummy specimen Sp1 and dummy specimen Sp2 should be explained by the joints, because dummy specimens are not subjected to any load.

The most exposed thermocouple from dummy specimen Sp3 never reached 300 ºC. The maximum temperature reached by thermocouple S4 was 86 ºC after 36 min of fire exposure, while the specimen Sp2 only reached 81 ºC after the same time.

The temperature of the GLT columns from specimens Sp1 and Sp2 has a very similar trend; however, the timber column from specimen Sp3 has reached smaller temperatures for the same time of test, see Table 3 for a comparative time window. The double protection layer of Specimen Sp3 granted a very large plateau, below 100 ºC, increasing the fire resistance by 20 % when using the same load level of 36609 [N].

2.4. Displacement and load measurements

Displacement and load were measured during the experimental tests. The load was applied 10 min prior to the start of the fire and was stable in the range of + 5 %, + 16 % and + 8 % with respect to the target value, respectively to specimens Sp1, Sp2 and Sp3, with the exception at the end of the test, when the hydraulics had difficulties keeping the load level due to the high level of the rate of displacement. Fig. 6 shows the load level for each fire test and the vertical contraction displacement over time (depicted as positive), assuming zero displacement at the beginning of the heating phase of each fire test.

The shape of the vertical contraction displacement was similar to all the specimens. The test ended with a sharp increase in the vertical contraction displacement rate. The criterion that defined the fire resistance was the displacement rate for all specimens, but the limiting vertical contraction was very close, see Table 4. The fire resistance is defined in completed minutes.

The failure mode was identified by flexural buckling along the strong axis due to the restraining effect of both supports. The localised effect of the load was also verified due to the existence of the drilled hole on the top of the column used to apply the load on a steel shaft. Moreover, there might have been some loss of fire integrity at the top support, allowing for fast charring in this region, producing some extra charring and some delamination between the lamellas. Fig. 7 shows the residual cross-section of each GLT timber column after the test.

3. Finite element model

The finite element model is a full 3D solid finite element model for thermal and mechanical analysis, allowing for some heat conduction along the length of the element.

The computational model includes four different types of analyses. The first one (analysis 1) is the elastic buckling analysis (important to compare the elastic buckling load and the first mode of instability that was used to include the geometric imperfection). This solution process uses the Block Lankzos extraction method. The second simulation (analysis 2) is a Geometrically and Materially Non-linear Imperfection Analysis (GMNIA) to determine the load-bearing capacity of the timber column at room temperature. This solution process is incremental in force (ΔF=5000 N, with the possibility to reduce ΔF to 0.1 N) and iterative, and uses the Newton-Raphson method. The convergence of the iterative process is based on the control of the displacement, using a tolerance of 10^{-3} and a reference value of 1 m. The third simulation (analysis 3) used a transient nonlinear analysis (TNA) to determine the temperature field during the fire exposure. This solution is also incremental in time (Δt=60 s, with the possibility to reduce Δt to 1 s) and iterative. The convergence is based on the calculation of the heat flow, using a tolerance of 10^{-3} and a reference value of 10^{-6} W. The fourth simulation (analysis 4) is a thermo-mechanical analysis, based on GMNIA that includes the effect of the mechanical load and fire in order to determine the fire resistance. This process is incremental in time (Δt=10 s, with the possibility to reduce Δt to 0.00001 s) and iterative. The convergence is based on displacement control, using a tolerance of 10^{-3} and a reference value of 1 m.

3.1. Material properties

The thermal properties are temperature-dependent for all the materials involved in the thermal simulations (timber [2], Gypsum plasterboard [2], and steel [21]). Fig. 8 presents the main thermal properties for all the materials involved, with the exception of the emissivity of the radiation-exposed material (gypsum, $\varepsilon = 0.8$).

The mechanical properties are temperature and fibre-dependent. Wood is an anisotropic material, due to the way the natural growth pattern and cellular structure of the tree. The wood model considers different behaviour of the material in the direction of the fibers, radial direction, and tangential direction. The strength and stiffness of wood are considerably higher in the longitudinal than in the other orthogonal directions. The generalised Hooke law for an orthotropic material is considered. Table 5 gives the values used for the elastic behaviour of the material. This material model considers the reduction coefficient for elevated temperatures, assuming 1 % of the room temperature values for residual strength and stiffness at 300 ºC and temperatures above. Moreover, according to prEN1995–1–2 [2], it is possible to conclude that the compressive strength of wood in the direction parallel to the grain (direction x) is linearly reduced with increasing temperature. The modulus of elasticity (EX, EY, EZ) is also affected by the increase in temperature, applying the reduction factors between 100 and 300 ºC, see Fig. 9.

Poisson's coefficients (ν_{XY}, ν_{YZ}, ν_{XZ}) are considered constant with increasing temperature, in accordance with the current version of the EN1995–1–2 [1] and the next generation [2] that do not define correction factors to be applied for this property.

The transverse elastic modulus (G_{XY}, G_{YZ}, G_{XZ}) also undergoes a reduction with increasing temperature, and the same reduction coefficients of the modulus of elasticity are used, since both elastic properties of wood are related through Poisson's coefficients. The failure of wood can be presented in several ways, such as fibre breakage, microcracking of the matrix, detachment of fibres or delamination. To characterise this effect, the Hill criterion is adopted [7]. This criterion is based on von Mises's theory and adapted for orthotropic materials. Hill's criterion considers the interaction between the stress in the failure mechanism and depends on the orientation of the stress with respect to the orthotropic axis of the material. This criterion allows the determination of the elastic and elastoplastic zones in the stress-strain relationship of the wood. The characteristic parameters of the orthotropic material, defined for this criterion, are the R_{ij} yield rates, which are established as a function of the limit stress in the main directions of the material. Assuming that the wood does not have the plastic capacity, the elastic-plastic regime is considered for the constitutive law in this investigation, just to ensure that the material remains in the elastic limit. The compressive strength $f_{xx}^{y} = f_{c,0,g,k}$ was experimentally measured at

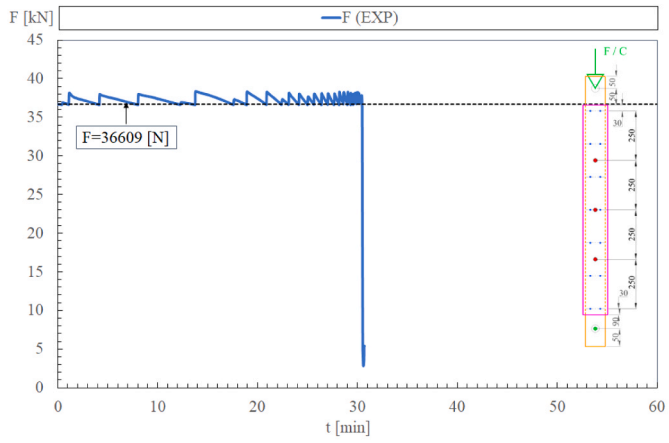

a) Load in specimen Sp1.

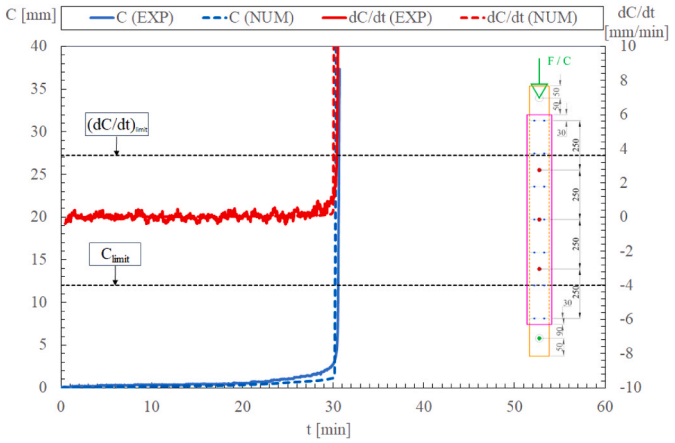

b) Displacement and rate of displacement in specimen Sp1.

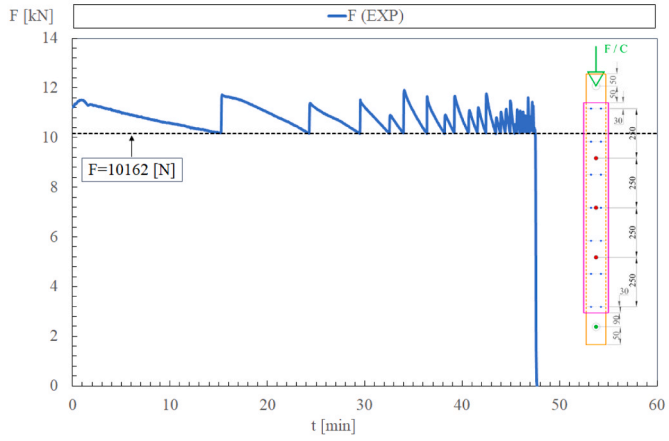

c) Load in specimen Sp2.

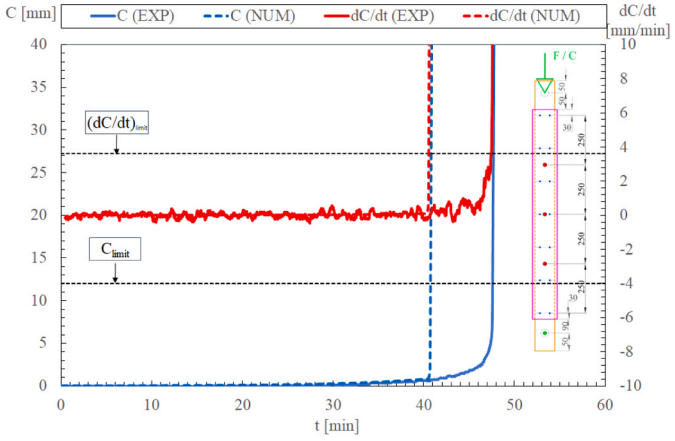

d) Displacement and rate of displacement in specimen Sp2.

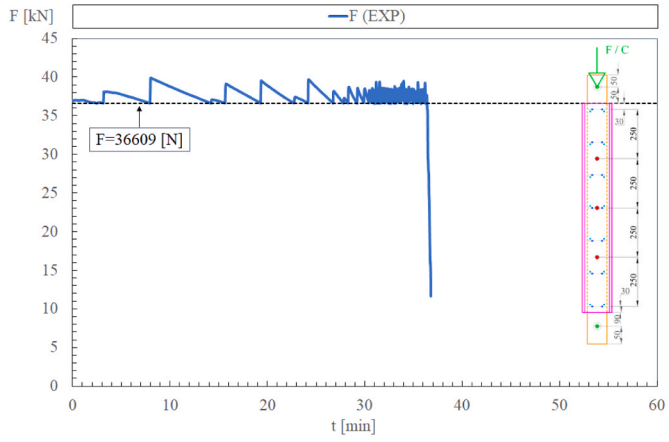

e) Load in specimen Sp3.

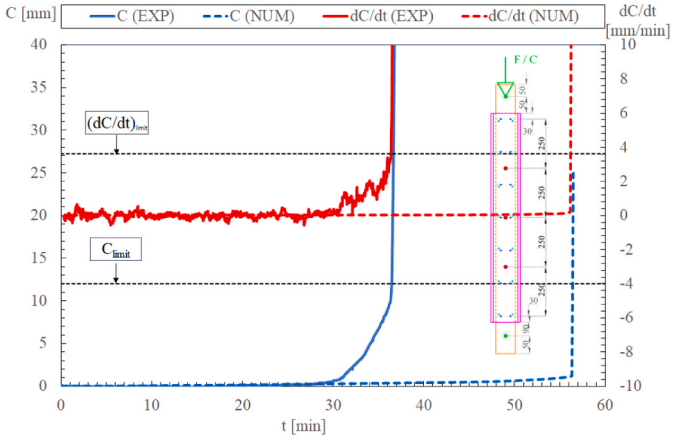

f) Displacement and rate of displacement in specimen Sp3.

Fig. 6. Load and rate of vertical displacement (contraction) during the time of test for all the specimens.

Table 4
Fire resistance. Experimental results according to EN1363-1 [18].

Specimen	Load [N]	Layers/ thickness [mm]	$C_{limit} = h/100$ [min]	$(dC/dt)_{limit} = (3h/1000)$ [min]	Fire resistance (EXP) [min]
Sp1	36609	1/ 12.5	30.52	30.39	30
Sp2	10162	1/ 12.5	47.60	47.42	47
Sp3	36609	2/ 12.5	36.47	36.38	36

a) Specimen Sp1. b) Specimen Sp2. c) Specimen Sp3.

Fig. 7. Residual cross-section of all specimens after fire test.

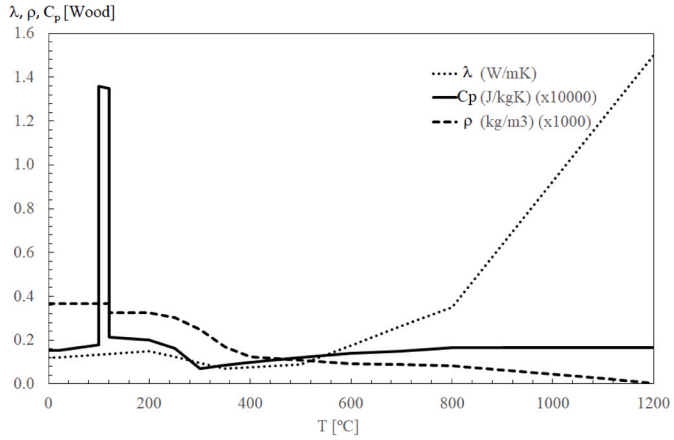

a) wood (prEN1995-1-2), [2].

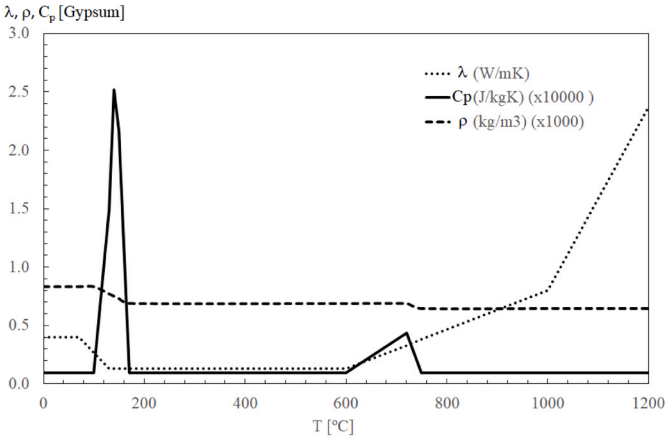

b) Gypsum plasterboard (prEN1995-1-2), [2].

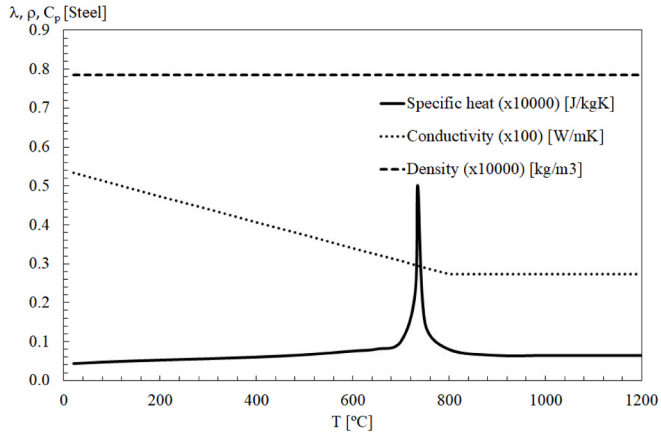

c) Steel (EN1993-1-2), [21].

Fig. 8. Temperature-dependent thermal properties for wood, gypsum and steel used in the numerical models.

Table 5
Linear elastic orthotropic properties for softwood Spruce Sitka [22].

	20 °C	100 °C	300 °C
E_X (MPa)	11500	4025	115
E_Y (MPa)	897	313	8
E_Z (MPa)	494	173	4
ν_{XY}	0.372	0.372	0.372
ν_{YZ}	0.435	0.435	0.435
ν_{XZ}	0.467	0.467	0.467
G_{XY} (MPa)	736	257	7
G_{YZ} (MPa)	34	12	0.3
G_{XZ} (MPa)	701	245	7

room temperature (26 MPa), but the standard EN14080 [20] establishes a minimum value of 24 MPa.

Table 6 gives the yielding rates used for each orthogonal direction and temperature level.

3.2. Numerical results

The mesh does not change between simulations, with the exception of analysis 3, which introduces the fire protection material. The gypsum plates are used solely for fire protection and contribute directly to the thermal simulation (analysis 3) and indirectly to the thermo-mechanical simulation (analysis 4). Fig. 10 shows the mesh used for each simulation process and presents some important results. The average element size is

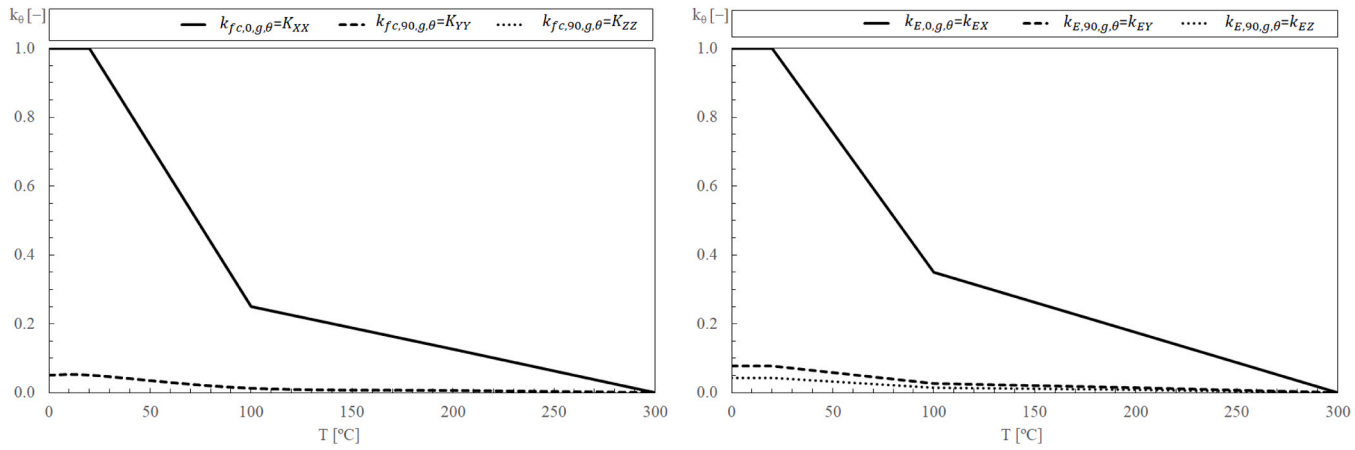

a) Reduction factors for the compressive strength in the three main directions of orthotropy.

b) Reduction factors for the Elastic modulus in the three main directions of orthotropy.

Fig. 9. Temperature-dependent mechanical properties of for this wood used in the numerical models.

Table 6
Strength limit in tension and Hill coefficients for softwood Spruce Sitka [23].

	20 °C	100 °C	300 °C
f^y (MPa)	24	6	0.24
$R_{XX}=f^y_{xx}/f^y$	1	1	1
$R_{YY}=f^y_{yy}/f^y$	0.052	0.052	0.052
$R_{ZZ}=f^y_{zz}/f^y$	0.052	0.052	0.052
$R_{XY}=f^y_{xy}/\left(\frac{f^y}{\sqrt{3}}\right)$	0.405	0.405	0.179
$R_{YZ}=f^y_{yz}/\left(\frac{f^y}{\sqrt{3}}\right)$	0.405	0.405	0.179
$R_{XZ}=f^y_{xz}/\left(\frac{f^y}{\sqrt{3}}\right)$	0.405	0.405	0.179

5 mm. Fig. 10a presents the first mode of instability associated with a critical load of 481 kN. Fig. 10b represents the von Mises stress for the last equilibrium position, corresponding to the load bearing capacity of 172 kN. Fig. 10 c) illustrates the mesh and temperature field at the 30-minute time. It can be noted that the protection effect of a 12.5 mm gypsum layer, keeping the residual area below 300 °C with a dimension of 60 % of the original cross-section for time 30 min, and 55 % of the original cross-section for time corresponding to 31.8 min.

Two main types of finite elements were used. For analyses 1, 2 and 4, the eight-node solid finite element (SOLID185) was selected. This element has 8 nodes, each with three degrees of freedom (three translations in each spatial direction). The element uses linear interpolating functions and an enhanced strain formulation for the integration method, preventing shear locking in bending-dominated problems and volumetric locking in nearly incompressible cases. The mesh only includes hexahedral shape finite elements. The initial imperfection was introduced in the model to account for accidental eccentricities, out-of-straightness, and other imperfections. The first instability mode was used to define the imperfect shape of the member, assuming a maximum initial deviation from straightness of L/500 [24].

For analysis 3, the eight-node solid finite element (SOLID70) was selected for the thermal analysis. This element has 8 nodes, each with one degree of freedom (temperature). The element uses linear interpolating functions and the full Gauss integration method. The mesh only includes hexahedral shape finite elements.

The analysis 4 used the same mesh as analysis 2, including the transient results from the analysis 3.

The critical buckling load determined by ANSYS was also compared with the Euler formula, assuming the material as isotropic, with the mean elastic modulus in the direction parallel to grain $E_{0,g,mean}$. The result is very close with a relative difference of 4 %. The maximum load-bearing capacity at room temperature for this wood species and grade GL24h was determined to be 172 kN, which is very close to 180 kN as determined by the simplified method (4 % relative difference). The fire resistance was also determined for the specimen Sp1, achieving the last equilibrium position at 30 min (0 % relative difference, corresponding to an absolute difference of 0 min).

3.3. Validation and verification

The verification of analysis 1 achieved a relative difference of 4 % for the case of GL24h, with a cross-sectional area of 80 × 100 mm² and a length of 1.2 m. The bigger difference (5.9 %) was determined for the case of GL24h, with a cross-sectional area of 140 × 160 mm² and a length of 2.4 m and is mainly due to the orthotropic behaviour. The comparison of the results was also determined for other cross-sections, lengths and material grades.

The verification of analysis 2 for the load-bearing result achieved a relative difference of 5 % for the case of GL24h, with a cross-sectional area of 80 × 100 mm² and a length of 1.2 m. The bigger difference (8 %) was determined for the case of GL24h, with a cross-sectional area of 140 × 160 mm² and a length of 2.4 m. The comparison of the results was also determined for other cross-sections, lengths and material grades.

The validation of analysis 3 for the temperature results was determined for the predicted temperatures inside the cross-section (dummy) and for the temperature predicted in the external surface of the timber element (below the gypsum protection). The validation was determined by the calculation of the Root Mean Square Error (RMSE), using a time increment of 2.5 min. The maximum RMSE was determined for the dummy Sp1 at the position S4 with 84 °C. The maximum RMSE for the temperature predictions on the external surface of the timber element (Specimen Sp1) was 36°C for the position S11. The maximum RMSE was determined for the dummy Sp2 at the position S2 with 202 °C. The minimum RMSE was determined for the position S1 with 7.5 °C. The maximum RMSE was determined for the position S13 with an average difference of 83 °C. After 25 min, the numerical results are over-predicting the temperature in comparison to the experimental measurements, see Fig. 5c). This may explain the smaller fire resistance

a) Analysis 1: Elastic buckling analysis (first buckling mode, Fcr= 481393 N)

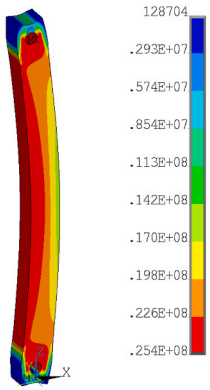

b) Analysis 2: GMNIA for load bearing capacity (172380 N), (von Mises stress Pa).

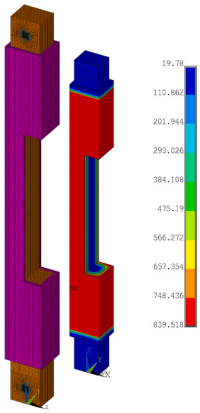

c) Analysis 3: TNA for temperature field, (time= 30 min) (temperature ºC on the residual cross-section).

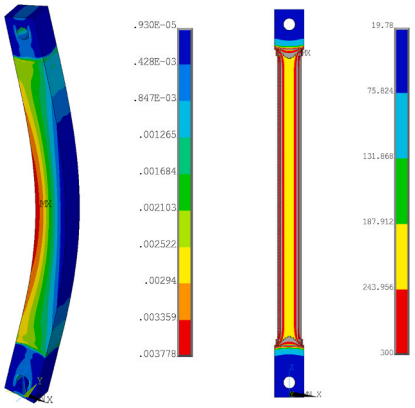

D) Analysis 4: GMNIA for fire resistance (time= 30 min (Total mechanical strain [-]) (Residual elements below 300 ºC.

Fig. 10. Example of results during simulations for the case of Specimen Sp1.

determined by the numerical results in comparison to the experimental results, see Fig. 6d). The maximum RMSE was also determined for the dummy Sp3 at position S3 with 9.4 ºC. The maximum RMSE for the external surface of the timber column (Specimen S3) was determined by 16.5 ºC at the position S12. Because the failure mode was identified by the separation of the lamellas, the fire resistance obtained by the

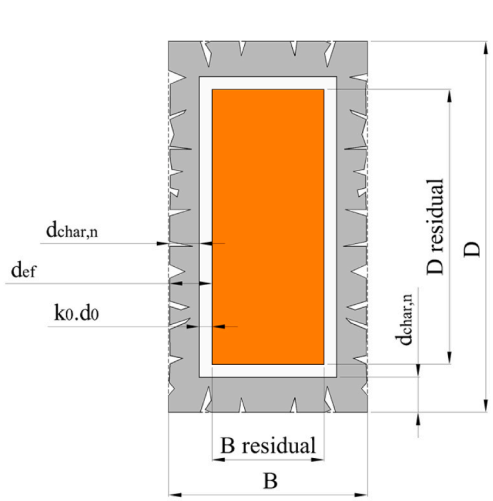

a) Unprotected timber elements.

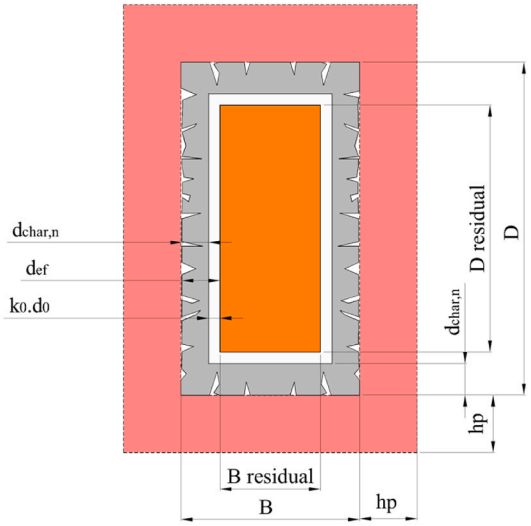

b) Protected timber elements.

Fig. 11. Charring model according to EN1995–1–2 [1].

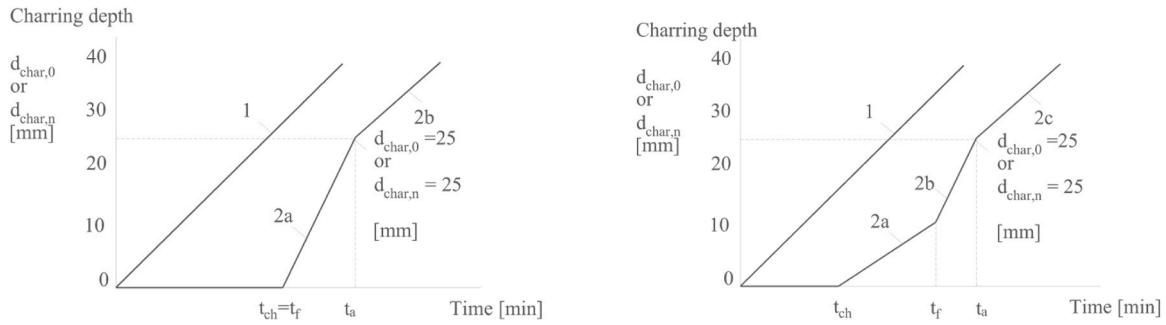

a) Case when $t_f = t_{ch}$ b) Case when $t_{ch} < t_f$.

Fig. 12. Charring depth depending on the time of fire exposure, EN1995–1–2 [1].

experimental results is quite smaller than the fire resistance determined by the numerical model, see Fig. 6 f).

The validation of analysis 4 to determine the fire performance was made by predicting the relative difference for the critical time and the calculation of the RMSE for the axial contraction displacement for each specimen. The relative difference is only presented for the specimens Sp1 and Sp2, because they had the same failure mode (flexural buckling). The relative difference was 0 % and 17.5 % for Specimens Sp1 and Sp2, respectively. The bigger difference obtained for specimen Sp2 is related to the over-prediction of the temperature in the cross-section after 25 min. The comparison of the contraction axial displacement gives an RMSE of 0.55 mm for the specimen Sp1, and 0.35 mm for Specimen Sp2, using the same time increment of 2.5 min. These values are almost below the required precision for the measuring equipment regarding displacement (±0.5 mm).

4. Simplified calculation method

The EN1995–1–2 [1] includes a design method based on an effective cross-section method that uses the ECM. The char depth is based on the

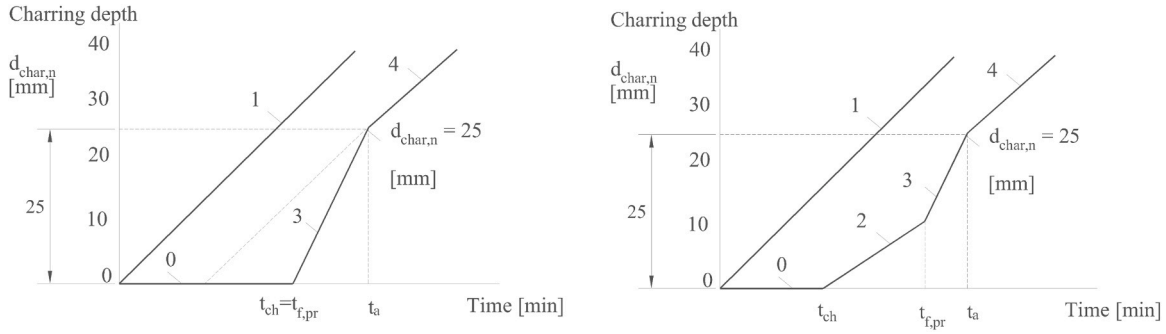

a) Case when $t_f = t_{ch}$, keeping the integrity. b) Case when $t_{ch} < t_f$, keeping the integrity.

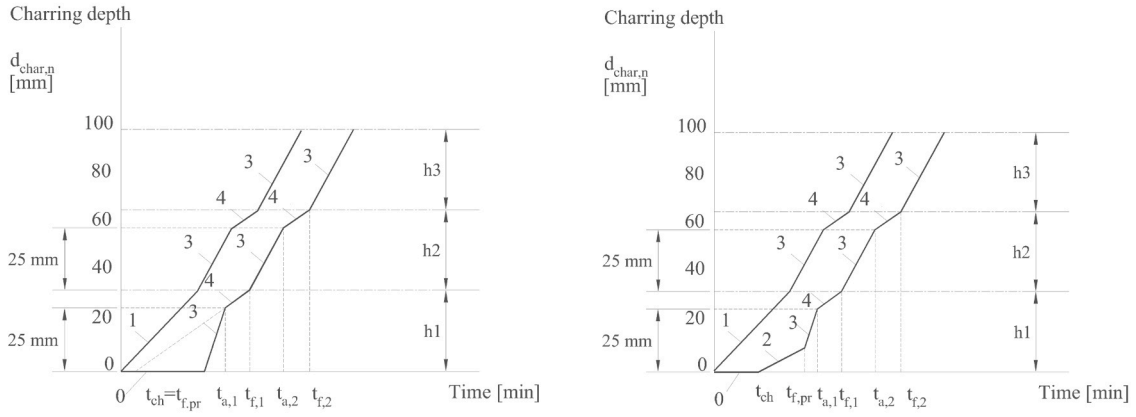

c) Case when $t_f = t_{ch}$, losing integrity. d) Case when $t_{ch} < t_f$, losing integrity.

Fig. 13. Charring depth depending on fire exposure time and integrity of the lamellas, prEN1995–1–2 [2].

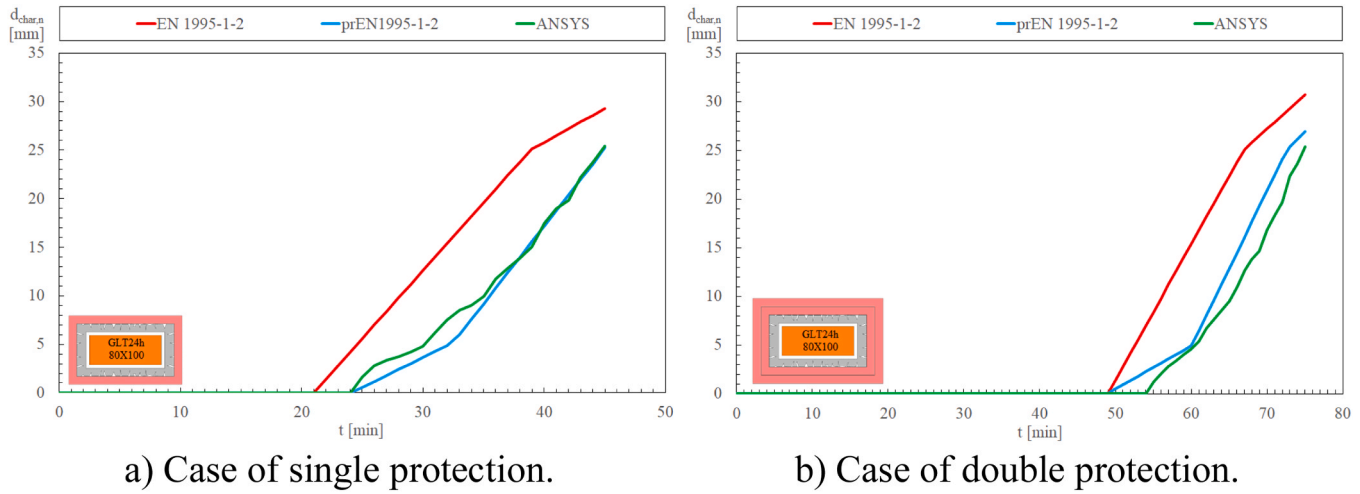

Fig. 14. Comparison of the charring models with the numerical results for the column 80 × 100, GL24h with different fire protection level.

notional char layer $d_{char,n}$ and a zero-strength layer to compensate for the loss of strength and stiffness of heated but uncharred wood $k_0 \times d_0$. The remaining effective cross-section has wood's strength and stiffness properties at room temperature and may be used to determine the load-bearing capacity of the element, see Fig. 11.

The notional char layer is determined by Eq. (1), assuming the required fire resistance time $t_{fi,req}$ and considering the 4 sides exposed to fire. The effective charring depth is determined by Eq. (2) and allows the calculation of the effective area. This area does not depend on the position of the lamellas, see Eq. (3).

$$d_{char,n} = t_{fi,req} \times \beta_n \tag{1}$$

$$d_{ef} = d_{char,n} + k_0 \times d_0 \tag{2}$$

$$\begin{aligned} B_{residual} &= B - 2 \times d_{ef} \\ D_{residual} &= D - 2 \times d_{ef} \end{aligned} \tag{3}$$

For the case of protected elements, one needs to determine if charring begins before or after the failure of the protection material. According to EN1995–1–2 [1], the failure time of the fire protection t_f and the start of charring t_{ch} may be determined by testing, or alternatively by EN1995–1–2 [1] or EN13381–7 [25]. Depending on the case, the notional char layer may be determined using different charring rates, according to EN1995–1–2 [1], see Fig. 12. Line 1 is dedicated to unprotected timber elements, and line 2 (2a, 2b and 2c) is dedicated to protected timber elements. Fig. 12 a) is the model for the case when the start of the charring coincides with the failure time of the protection material. Fig. 12 b) reflects the premature start of charring, before the failure of the protection material.

The next generation prEN1995–1–2 includes the design for GLT elements, considering two possibilities regarding the integrity of the bond surface between lamellas. If the bond surface integrity is maintained during the fire exposure, the notional char layer may be determined in a similar way to the previous method in the current version of EN1995–1–2. If the bond is not maintained during fire exposure, the notional char layer differs from the previous version, presenting new charring rates, considering the thermal effect of the lamellas, see Fig. 13 [2].

The notional design charring rate β_n should be calculated in accordance with Eq. (4) using the applicable modification factors for charring k_i and the basic design charring rate β_0. Eq. (5) and Eq. (6) is used to determine the residual cross-section. The factor k_{side} is the number of respective opposite sides exposed to fire.

$$\begin{aligned} d_{char,n} &= \sum_{phases} \beta_n \times \Delta t \\ \beta_n &= \prod k_i \times \beta_0 \end{aligned} \tag{4}$$

$$d_{ef} = d_{char,n} + d_0 \tag{5}$$

$$\begin{aligned} B_{ef} &= B - k_{side} \times d_{ef} \\ D_{ef} &= D - k_{side} \times d_{ef} \end{aligned} \tag{6}$$

For initially protected timber members, the next generation of the ECM [2] predicts several phases: the encapsulated phase (Phase 0), when no charring occurs behind the fire protection material; predicts the protected charring phase (Phase 2), when charring starts before the failure of the protection material (protection still in place); predicts the post-protected charring phase (Phase 3), when the failure of the protection material occurs and before a fully developed char layer has been formed; predicts the consolidated charring phase (Phase 4), usually after the 25 mm and before the lamellas thickness.

Fig. 14 shows the comparison of the 300 °C isothermal determined by ANSYS with the notional char layer determined by the current version of the EN1995–1–2 [1] and the next generation of the prEN1995–1–2 [2]. One can see that the numerical results are in good agreement with the ECM presented by the prEN1995–1–2 [2].

In any case of the design process following the current version of EN1995–1–2 [1] or the next version prEN1995–1–2 [2], the load-bearing capacity of the element under compression and fire depends on the expected failure mode (flexural buckling). If one assumes this failure mode, the load bearing capacity is defined by $N_{c,Rd,t,\,fi}$, following the procedure presented from Eq. (7) to Eq. (11), and depends on the reduction factor $k_{c,fi,z}$, on the residual area $A_{residual}$, and on the design compression strength in the principal fibre direction. The reduction factor $k_{c,fi,z}$ depends on the relative slenderness λ_{rel} and on the intermediate parameter k_z. The intermediate parameter depends on the imperfection factor β_c. The relative slenderness depends on the characteristic compression strength in the principal fibre direction and also on the fifth percentile value of modulus of elasticity.

$$N_{c,Rd,t,fi} = k_{c,fi,z} \times f_{c,0,d} \times A_{residual} \tag{7}$$

$$k_{c,fi,z} = \frac{1}{k_z + \sqrt{k_z^2 - \lambda_{rel}^2}} \tag{8}$$

$$k_z = 0.5\left(1 + \beta_c(\lambda_{rel} - 0.3) + \lambda_{rel}^2\right) \tag{9}$$

Table 7
Comparison of the numerical results with the simplified method.

Spec.	Cross-section [mm. mm]	Wood grade	Column Length [m]	Protection layer [#/mm]	$N_{b,Rd}$ ANSYS [N]	$N_{b,Rd}$ EN1995-1-1 [N]	t_{fi} ANSYS [min]				t_{fi} EN1995-1-2 [min]				t_{fi} prEN1995-1-2 [min]			
							Load level				Load level				Load level			
							6 %	12 %	21 %	36 %	6 %	12 %	21 %	36 %	6 %	12 %	21 %	36 %
P1	80 × 100	GL24h	1.2	1/12.5	172380	180871	40	35	30	24	36	33	30	27	38	35	33	27
P2	80 × 100	GL24h	1.2	2/12.5	172380	180871	70	63	56	47	64	61	58	55	65	63	61	53

$$\lambda_{rel} = \frac{\lambda}{\pi}\sqrt{\frac{f_{c,0,k}}{E_{0.05}}} \tag{10}$$

$$\lambda = \frac{L_e}{i_z} \tag{11}$$

The imperfection is also considered. For the Initial out-of-straightness between supports equal to L/500 (GLT), the imperfection factor to be used is $\beta_c = 0.1$.

The fire resistance of columns under fire decreases with the slenderness, as expected.

5. Comparison of results

The numerical results were compared with both simplified methods, the current version of EN1995–1–2 [1] and the next generation prEN1995–1–2 [2], for the case of single protection (1/12.5) and double protection (2/12.5), using different load levels (6, 12, 21 and 36 %) and different protection levels (single layer and double layer) see Table 7.

The fire resistance of the GL24h timber columns with a cross-section of 80 × 100 mm^2 was determined for single and double protection layers. The contraction displacement is presented for all simulations, showing the complete displacement from the start of the applied load. It is worth noting that the previous graphs presented for the axial contraction displacement, “as positive”, started with the axial contraction measured from the commencement of heating. In fact, according to EN1363–1 [18], and for vertical load-bearing elements, axial deflection should be expressed negatively whenever there is no thermal expansion, which is the case herein. The results presented in Fig. 15 are depicted from the staring of the mechanical load. There is an initial increasing load during the first 60 s that is reflected in the initial increasing vertical contraction, in order to increase the solution convergence.

The fire resistance decreases with the load level. Doubling the protection level from single protection to double protection layers, there is an increase in the fire resistance that depends on the load level. The increase changes from 70 % to 95 %, with the increase of the load level from 6 % to 36 %.

From Fig. 16, one can see that the numerical results are closer to the simplified results from the next generation prEN1995–1–2 [2], however, the numerical results overpredict the fire resistance for the lowest load level and underpredict for higher load levels, which may indicate that both simplified methods are still unsafe.

6. Parametric analysis

After verification and validation of the finite element model, more simulations were developed to analyse the effect of the timber grade material (GL24h, GL28h), the effect of the cross-section (100 ×120 mm^2, 140x160mm^2), the effect of the buckling length (L=1.2 m, L=2.4 m), and the effect of the load level (6, 12, 21 and 36 %), see Table 8. From the results presented, one can conclude that increasing the material grade will increase the fire resistance. On average, changing the material grade from GL24h to GL28h there is an increase of 6.4 % for shorter columns and 2.3 % for slender columns, when using the 100 × 120 cross-section. These average numbers increase to 12.1 % and 6.2 %, respectively, when using the 140 × 160 cross-section.

The effect of the load level is also important. When increasing the load level from 6 % to the other load levels (12, 21 and 36 %), there is an average decrease in fire resistance by 14.2 %, 31.9 % and 47.2 %, respectively.

7. Conclusions

This investigation has provided an important study on the fire resistance of protected glued-laminated timber (GLT) columns, focusing

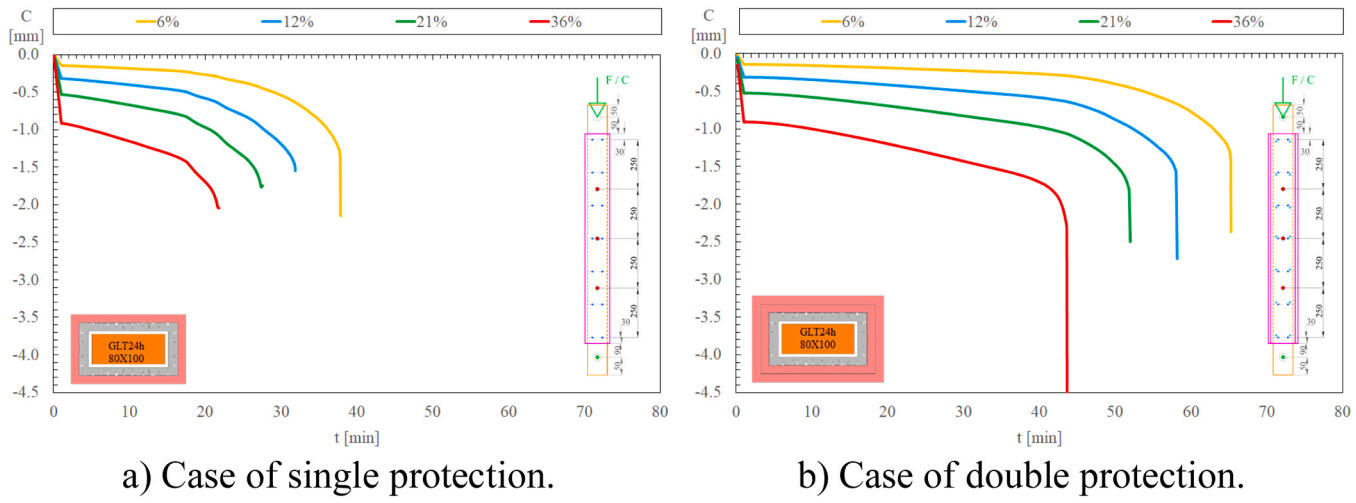

Fig. 15. Vertical axial contraction of timber column GL24h with different fire protection levels and load levels.

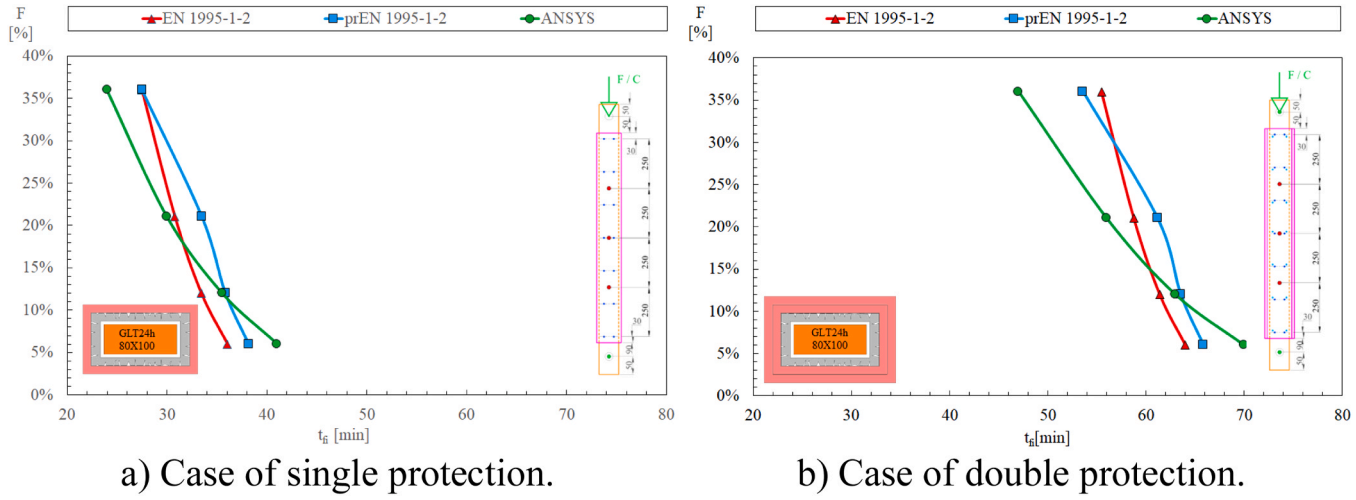

Fig. 16. Comparison of the fire resistance between the numerical results and the simplified methods.

Table 8
Parametric study: different columns protected with 1 gypsum layer.

Spec.	Cross-section [mm × mm]	Wood grade	Column Length [m]	Protection layer [#/mm]	$N_{b,Rd}$ ANSYS [N]	$N_{b,Rd}$ EN1995-1–1 [N]	t_{fi} ANSYS [min]			
							Load level			
							6 %	12 %	21 %	36 %
P3	100 × 120	GL24h	1.2	1/12.5	265168	278106	47	40	33	26
P4	100 × 120	GL24h	2.4	1/12.5	182848	196221	41	36	27	23
P5	100 × 120	GL28h	1.2	1/12.5	318198	323338	51	43	35	27
P6	100 × 120	GL28h	2.4	1/12.5	208992	218608	43	36	27	24
P7	140 × 160	GL24h	1.2	1/12.5	516292	530359	60	51	43	30
P8	140 × 160	GL24h	2.4	1/12.5	436422	474508	54	47	36	27
P7	140 × 160	GL28h	1.2	1/12.5	593780	617634	67	57	48	34
P8	140 × 160	GL28h	2.4	1/12.5	503469	544795	57	50	38	29

on the effects of geometry, load level, and gypsum-based cladding protection. The combination of experimental tests (limited to one cross-section, two load levels, and two protection levels), the use of 3D finite element modelling, and comparison with simplified design methods has led to several key conclusions:

1- Fire Protection effect: The application of gypsum plasterboard cladding significantly improves the fire resistance of GLT columns, acting as a thermal barrier that delays temperature rise and charring of the timber. Doubling the gypsum protection layer thickness notably increases fire resistance by approximately 70–95 %, with the increase of the load level from 6 % to 36 %. This confirms gypsum cladding as an effective fire protection system for timber columns.

2- Load Level effect: The fire resistance of timber columns decreases as the applied load level increases. The study quantified this reduction, showing that increasing the load from 6 % to 36 % of the ultimate capacity reduces fire resistance by nearly 47.2 %. This emphasises the

importance of considering load level in fire design assessments.

3- Material Grade and Cross-Section Effects: Higher timber material grades (e.g., GL28h compared to GL24h) enhance fire resistance, with increases up to 12 % observed for larger cross-sections. Larger cross-sectional dimensions and shorter column lengths also contribute positively to fire resistance, indicating that geometry and material quality are crucial parameters in fire safety design.

4- Numerical Modelling Verification and Validation: The developed full 3D solid finite element model, incorporating orthotropic, temperature-dependent material properties and nonlinear thermo-mechanical behaviour, accurately predicted temperature evolution, displacement, and char depth. The model showed good agreement with experimental results, with relative differences in critical parameters generally below 18 %, validating its use for fire performance prediction of timber columns.

5- Simplified Design Methods: The comparison with the current EN1995–1–2 and the upcoming prEN1995–1–2 simplified methods revealed that numerical results align more closely with the next-generation standard. However, discrepancies remain, especially at varying load levels, suggesting that simplified methods might still be unsafe or conservative in certain scenarios. This highlights the need for further refinement of design codes to incorporate load effects and protection integrity more accurately.

6- Failure Modes and Protection Integrity: The study observed that failure modes under fire include flexural buckling and debonding between lamellas. Maintaining the integrity of adhesive bonds during fire exposure is essential, as it impacts charring rates and load-bearing capacity. The choice of adhesive and its fire performance also affects the overall fire resistance of GLT columns.

In summary, this research substantiates that gypsum-based fire protection significantly enhances the fire performance of GLT timber columns, but fire resistance is highly sensitive to load level, material grade, and column geometry. The validated 3D finite element model provides a robust computational model for detailed fire safety assessment, bridging the gap between experimental data and design standards. Future design codes should incorporate these findings to improve safety and optimise the use of timber in sustainable construction.

These conclusions provide valuable insights that support the expanded and safer use of engineered timber in modern architecture, while addressing critical fire safety concerns.

CRediT authorship contribution statement

Abdelhamid Bouchaïr: Writing – review & editing, Supervision. **Loïc Lannou:** Validation, Investigation. **Javier Sánchez-Haro:** Writing – review & editing, Investigation, Conceptualization. **Ana B. Ramos-Gavilán:** Writing – review & editing, Investigation, Conceptualization. **Manuel D. Lorenzo:** Writing – review & editing, Investigation, Conceptualization. **Piloto Paulo A. G.:** Writing – review & editing, Writing – original draft, Supervision, Methodology, Investigation, Conceptualization.

Declaration of Competing Interest

The authors declare that they have no known competing financial interests or personal relationships that could have appeared to influence the work reported in this paper.

References

[1] CEN. Eurocode 5: Design of timber structures - Part 1-2: General - Structural fire design. Brussels: CEN. CEN - European Committee for Standardization; 2004.
[2] CEN, pr EN 1995-1.2. Eurocode 5: Design of timber structures - Part 1-2: General - Structural fire design. Brussels: CEN. CEN - European Committee for Standardization; 2023.
[3] Young SA, Clancy P. Compression mechanical properties of wood at temperatures simulating fire conditions. Fire Mater 2001;25(3):83–93. https://doi.org/10.1002/fam.759.
[4] Ali F, Kavanagh S. Fire resistance of timber columns. J Inst Wood Sci Oct. 2005;17(2):85–93. https://doi.org/10.1179/wsc.2005.17.2.85.
[5] Schnabl S, Turk G, Planinc I. Buckling of timber columns exposed to fire. Fire Saf J Oct. 2011;46(7):431–9. https://doi.org/10.1016/j.firesaf.2011.07.003.
[6] Mascia NT, Simoni RA. Analysis of failure criteria applied to wood. Eng Fail Anal Dec. 2013;35:703–12. https://doi.org/10.1016/j.engfailanal.2013.07.001.
[7] H. Rodney and R. Soc, A theory of the yielding and plastic flow of anisotropic metals, May 1948. doi: https://doi.org/10.1098/rspa.1948.0045.
[8] H.L. Malhotra and B.F. Rogowski, Fire resistance of laminated timber columns (Fire Research Note No. 671), London, 1967.
[9] Silva L, Alves M, Andrade D, Macanjo Ferreira D, Piloto P, Mesquita L. Tensile shear strength of wood adhesives with fire-retardants under elevated temperatures. vol. 0, no. 0 J Adhes Sci Technol Sep. 2025:1–23. https://doi.org/10.1080/01694243.2025.2563910.
[10] Gernay T. Fire resistance and burnout resistance of timber columns. Fire Saf J Jun. 2021;122(December 2020):103350. https://doi.org/10.1016/j.firesaf.2021.103350.
[11] Barber D, Schulz J, O'Loughlin E. Simplified engineering method to establish structural adequacy of mass timber columns for full fire duration. World Conf Timber Eng 2025 2025:227–36. https://doi.org/10.52202/080513-0029.
[12] Khelifa M, Thi VD, Oudjène M, Khennane A, El Ganaoui M, Rogaume Y. Modelling the response of timber beams under fire. Int J Civ Eng Sep. 2024;22(9):1537–49. https://doi.org/10.1007/s40999-024-00973-2.
[13] Li X, Yue K, Zhu L, Lv C, Wu J, Wu P, Li Q, Xu C, Sun K. Relationships between wood properties and fire performance of glulam columns made from six wood species commonly used in China. Case Stud Therm Eng Feb. 2024;54(July 2023):104029. https://doi.org/10.1016/j.csite.2024.104029.
[14] Huang J, Wang L. Experimental and Numerical Study on Progressive Collapse of the Midcolumn in a Glulam Timber Frame Exposed to Fire. Fire Sep. 2023;6(10):374. https://doi.org/10.3390/fire6100374.
[15] Han T, Tesfamariam S. Reliability analysis of timber columns under fire load using numerical models with equivalent section temperature. Eng Struct Feb. 2025;324(ember 2024):119345. https://doi.org/10.1016/j.engstruct.2024.119345.
[16] Zmaha MI, Pozdieiev SV, Zmaha YV, Nekora OV, Sidnei SO. Research of the behavioral of the wooden beams with fire protection lining under fire loading. IOP Conference Series Materials Science Engineering Jan. 2021;1021(1):012031. https://doi.org/10.1088/1757-899X/1021/1/012031.
[17] Korolchenko DA, Portnov FA. Study on structural fire protection and fire resistance of glued laminated timber columns. Buildings Dec. 2024;14(12):4049. https://doi.org/10.3390/buildings14124049.
[18] CEN. EN 1363-1: Fire resistance tests Part 1: General Requirements. Brussels: CEN. CEN - European Committee for Standardization; 2020. p. 52.
[19] CEN. EN 1365-4: Fire resistance tests for loadbearing elements. Part 4: Columns (\). Brussels: CEN. CEN - European Committee for Standardization; 2000.
[20] CEN. EN 14080 - Timber structures — Glued laminated timber and glued solid timber — Requirements. CEN 2013;(June):1–110.
[21] CEN. *EN 1993-1-2: Eurocode 3: Design of steel structures - Part 1-2: General rules - Structural fire design.* CEN-Europ. Brussels: CEN- European Committee for Standardization; 2005.
[22] USA - Department of Agriculture (Forest Service), Wood Handbook, 2010.
[23] T.H. Milhan, Numerical study on wooden beams subjected to high temperatures (in Portuguese), Instituto Politécnico de Bragança (MSc thesis), 2020.
[24] CEN. Eurocode 5: Design of timber structures - Part 1-1: General - Common rules and rules for buildings. Brussels: CEN. CEN - European Committee for Standardization; 2004. p. 1–123.
[25] CEN. EN 13381-7 Test methods for determining the contribution to the fire resistance of structural members. Part 7: Applied protection to timber members. Brussels: CEN. CEN - European Committee for Standardization; 2019.